

Supplementary Electronic Information for:

Nanotoxicity of polyelectrolyte-functionalized titania nanoparticles on microalgae and yeast: Role of the particle concentration, size and surface charge

Mohammed J Al-Awady^a, Gillian M Greenway^a and Vesselin N. Paunov^{*, a}

^a Department of Chemistry, University of Hull, Hull, HU67RX, UK.

Email for correspondence: V.N.Paunov@hull.ac.uk

Submitted to RSC Advances as a paper

8 Dec 2014

Typical TiO₂NPs particle size distribution

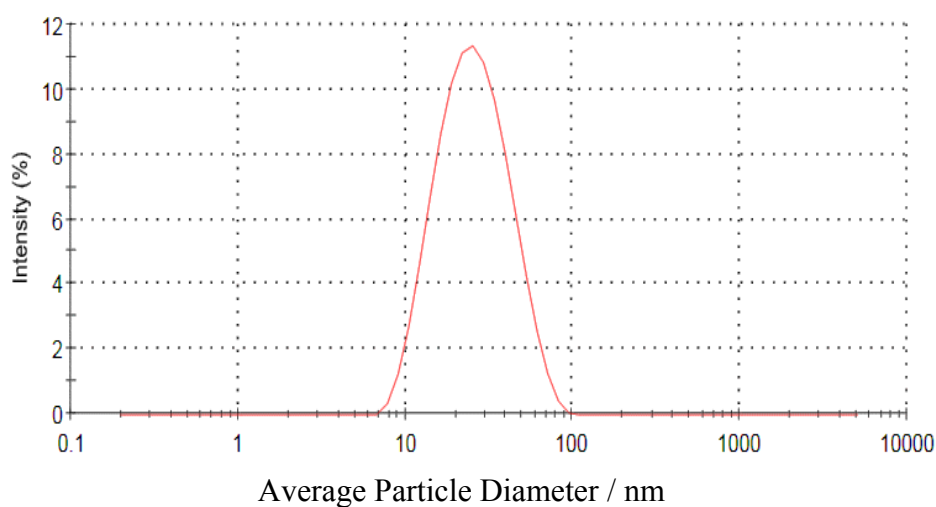


Figure S1. The average size distribution of TiO₂NPs dispersed in water (pH 4) after being synthesized by hydrolysis and condensation of titanium isopropoxide in acidic medium for 20 hours at 70 °C followed by annealing of the titania powder at 100 °C.

In Figure S1, we present the particle size distribution of TiO₂NPs suspension obtained by dispersing a fixed amount of titania in Milli-Q water (at pH 4) after sonication at 30% amplitude for 5 minutes as described in the synthesis of TiO₂NPs in the experimental section. The average particle diameter of the dispersed sample was then measured using a Zetasizer Nano ZL (Malvern, UK).

UV-Vis Spectroscopy of Titania Nanoparticles

Anatase titania of 5.0 nm crystallite domain size was dispersed in water at pH 4 to yield TiO₂NPs of average diameter 25 nm. A UV-Visible spectrum was obtained for the TiO₂NPs dispersion between 200 nm to 700 nm. Figure S2 shows that the absorption edge of these nanoparticles was around 375 nm (dotted line) which lies in the near UV range with a band gap energy of 3.5 eV. This is larger than the band gap value of 3.2 eV for the bulk TiO₂ as the band gap of semiconductor depends on particle size due to quantum confinement effects.

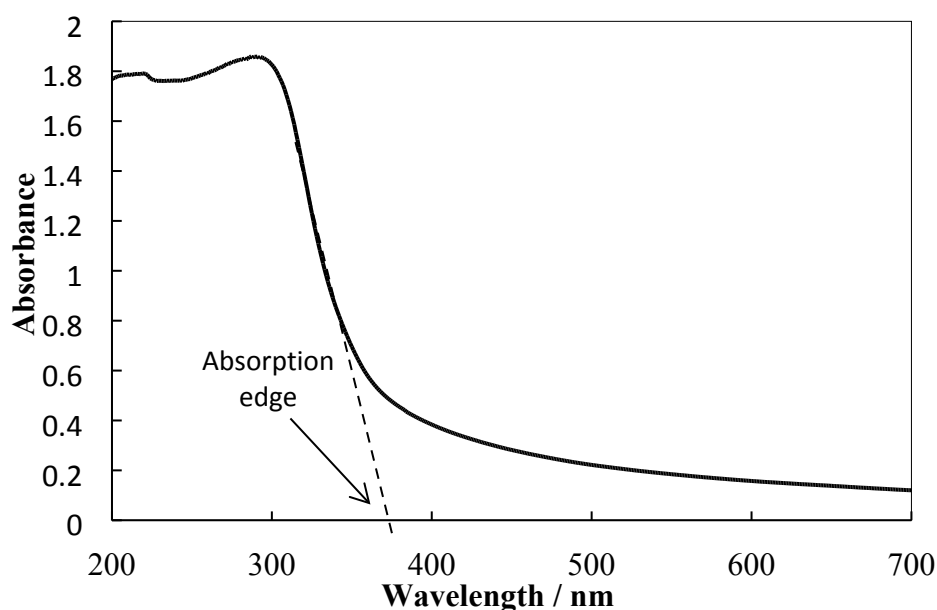


Figure S2. UV-Visible absorption spectrum of an aqueous dispersion of anatase TiO₂NPs of crystallite size 5 nm and average hydrodynamic radius 25 nm showing band gap energy 3.5 eV in comparison with 3.2 eV of bulk TiO₂. Dotted line that crosses the x-axis represent the absorption edge.

Effect of the calcination temperature of the synthesized titania nanoparticles on crystallite size

Once synthesized titanium dioxide nanoparticles were annealed at different temperatures (200°C - 800°C) using the Carbolite muffle furnace to find out the effect of temperature on the crystallite size of the nanoparticles. Figure S3 describes the powder X-ray diffraction patterns of the calcinated TiO₂ nanoparticles. Figure S3 (A, B, C, D, E and F) shows that the crystallite size of anatase TiO₂ becomes larger and the XRD bands ($2\theta \approx 25^\circ$) sharper, as the calcination temperature is increased resulting crystallite sizes for the TiO₂ of 6, 6.5, 7 and 12 nm, respectively. However, above 600°C, rutile TiO₂ peaks ($2\theta \approx 27^\circ$) started to appear as shown in Figures S3E and S3F. The above results are in agreement with analogous results previously reported in the literature.

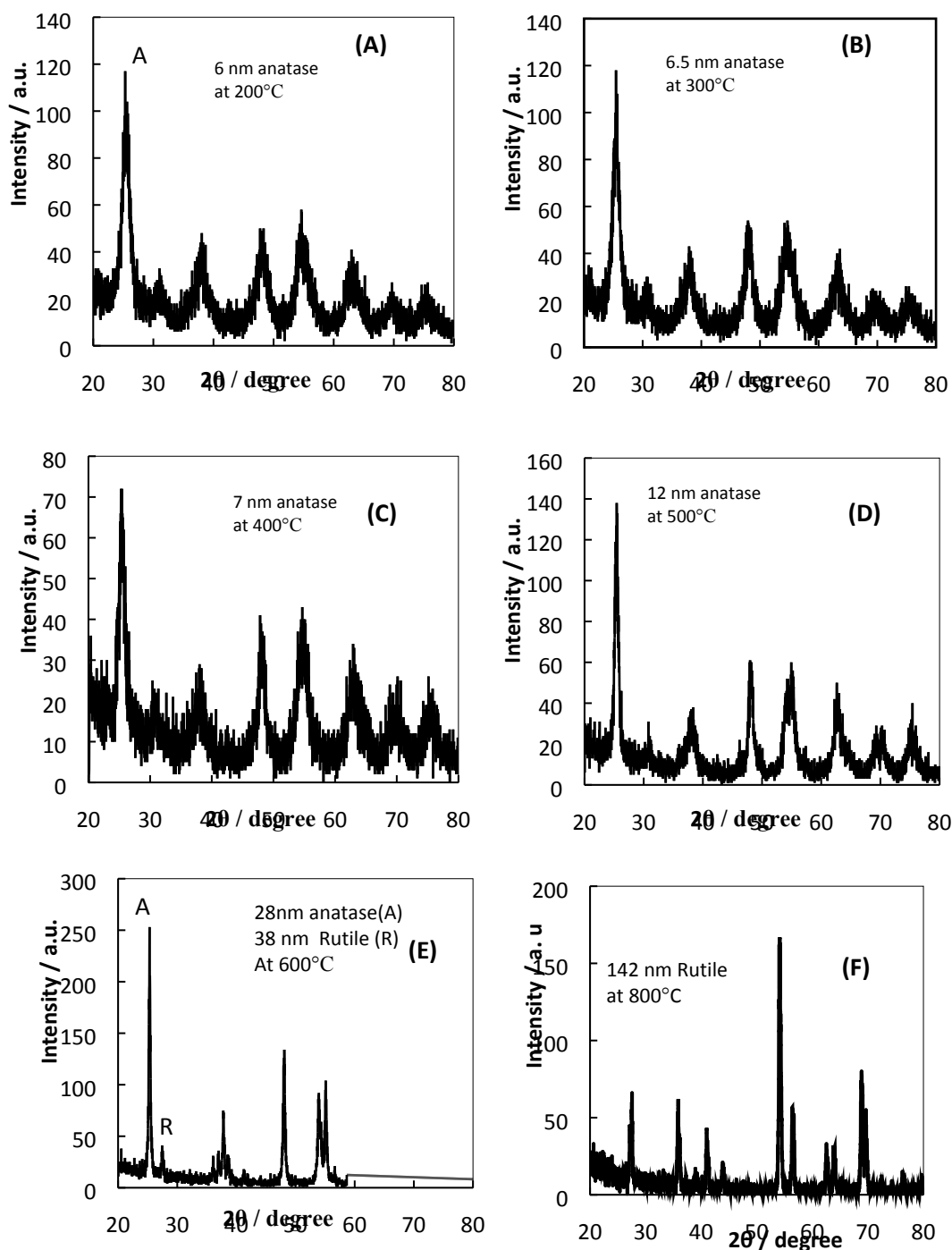
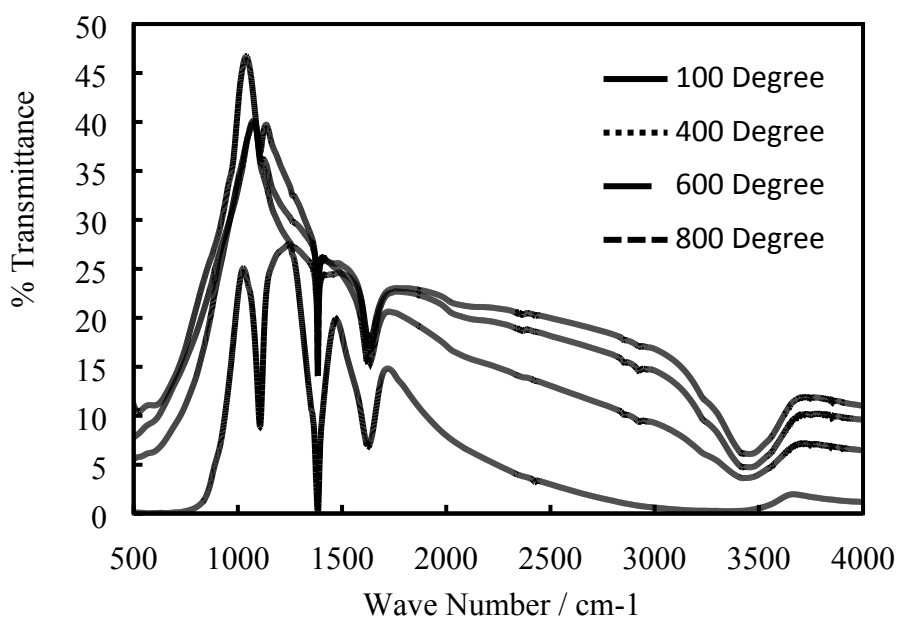


Figure S3: Powder X-Ray diffraction patterns of prepared TiO_2 nanoparticle at various calcination temperatures (A) 200°C, (B) 300°C, (C) 400°C, (D) 500°C, and (E) 600°C, showing formation of different sizes of anatase TiO_2 with sharper peaks as the temperature is increased from 200°C to 600°C (A, B, C, and D). However, with (E), the XRD peaks of anatase TiO_2 are very sharp (crystallite size 28 nm and 38 nm for anatase and rutile, respectively) while at 800 °C, rutile TiO_2 nanoparticles are dominant with 142 nm crystallite size.

Fourier Transform Infrared Spectroscopy (FTIR)

Fourier Transform Infrared Spectroscopy (FTIR) spectra were recorded at room temperature with a Perkin-Elmer FT-IR spectrometer-spectrum RX1. The FT-IR spectrometer was connected to a computer loaded with an IR Data Manager (IRDM) program. Samples of the annealed TiO₂ at 100, 400, 600 and 800 °C were pressed into discs using spectroscopically pure KBr. and spectra were obtained in the range 500-4000 cm⁻¹. Figure S4 shows very strong peaks at 500 cm⁻¹ - 650 cm⁻¹ which relate to the Ti-O bonding in for the anatase morphology. Moreover, the observed band at 1623 cm⁻¹ relate to stretching and vibration of the Ti-O-Ti group. The peaks at 1100 cm⁻¹, 3317 cm⁻¹ and 3352 cm⁻¹ correspond to stretching of absorbed water and hydroxyl group vibrations. However, at 600 °C the peak 1100 cm⁻¹ vanished which might be attributed to dehydration. Peaks at 2900-3000 cm⁻¹, correspond to the C-H stretching vibrations but these peaks disappeared at high temperature, which means all organic compounds were removed from the samples after the calcination. The sharp and intensive peak at 1385 cm⁻¹ is due to the presence of nitrates, which were added as HNO₃, during the



acidification of the solution in the sol-gel synthesis as a peptizing agent.

Figure S4: Fourier Transform Infrared Spectroscopy (FTIR) spectrum of annealed titania nanoparticles at 100, 400, 600 and 800 °C.

Thermogravimetry Analysis (TGA)

A TGA graph (A Mettler Toledo TGA/DSC1 with Star^e software system analyzer) of 20.1950 mg of anatase titania nanoparticles of crystallite size 5 nm is shown in Figure S5, illustrating the weight loss occurred in three steps. The first weight loss shows an endothermic peak at 100 °C to 180 °C due to the removal of absorbed water from the surface of sample. The second thermal degradation is from 180 °C to 325 °C due to the dehydration and combustion of organic species for example, residues of the precursor (Titanium Isopropoxide). The third degradation from 325 °C to 600 °C shows an extra weight loss which might be attributed to the phase transition corresponding with results from the XRD patterns and FTIR spectrum. Above 600 °C the sample mass remained constant at 84% representing the thermal stability of the sample.

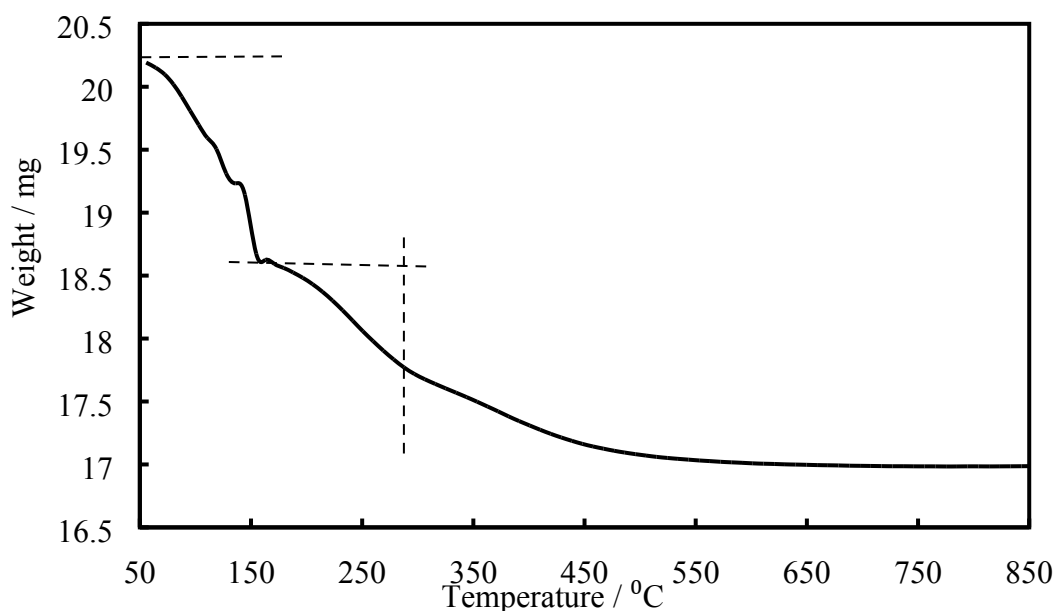


Figure S5: Thermal Gravimetric Analysis (TGA) graph of 5 nm anatase titania nanoparticles, showing three steps of thermal degradation: the first step represents dehydration, the second step refers to degradation of the organic compound and the last step is the phase transformation from anatase to rutile titania nanoparticles.

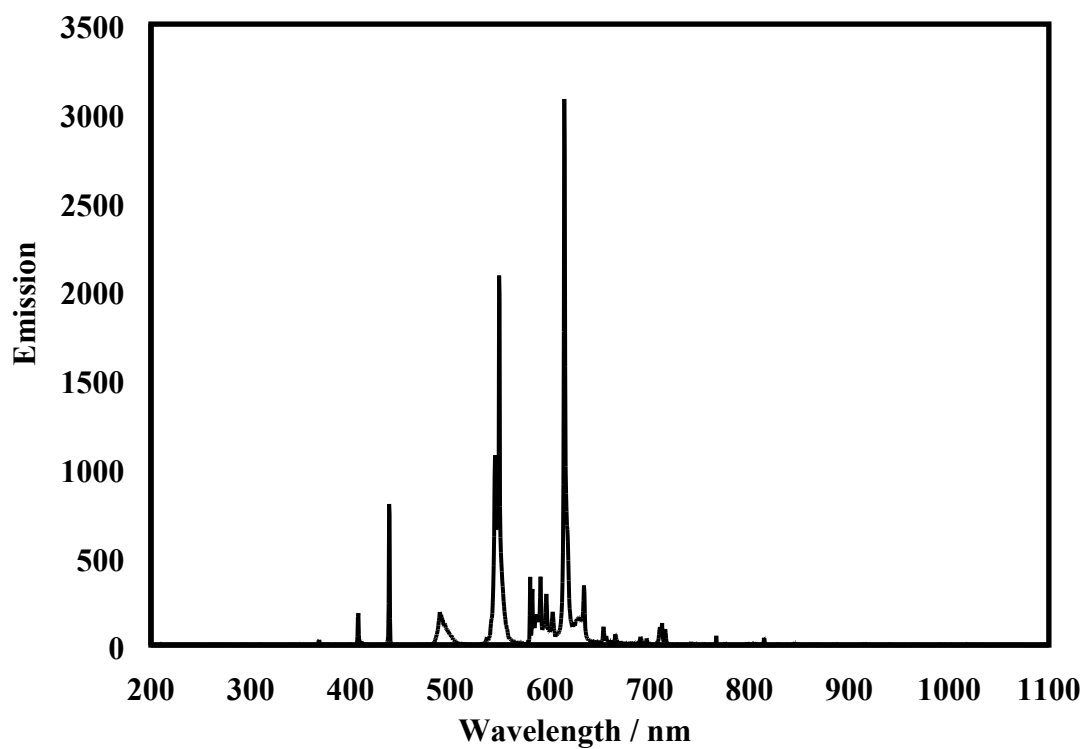


Figure S6: The emission spectrum of the visible light source which was used for irradiating *C. Reinhardtii* in the presence of TiO_2NPs at various exposure time which was measured by USB4000-UV-VIS detector (Toshiba TCD1304AP Linear CCD array, USA).

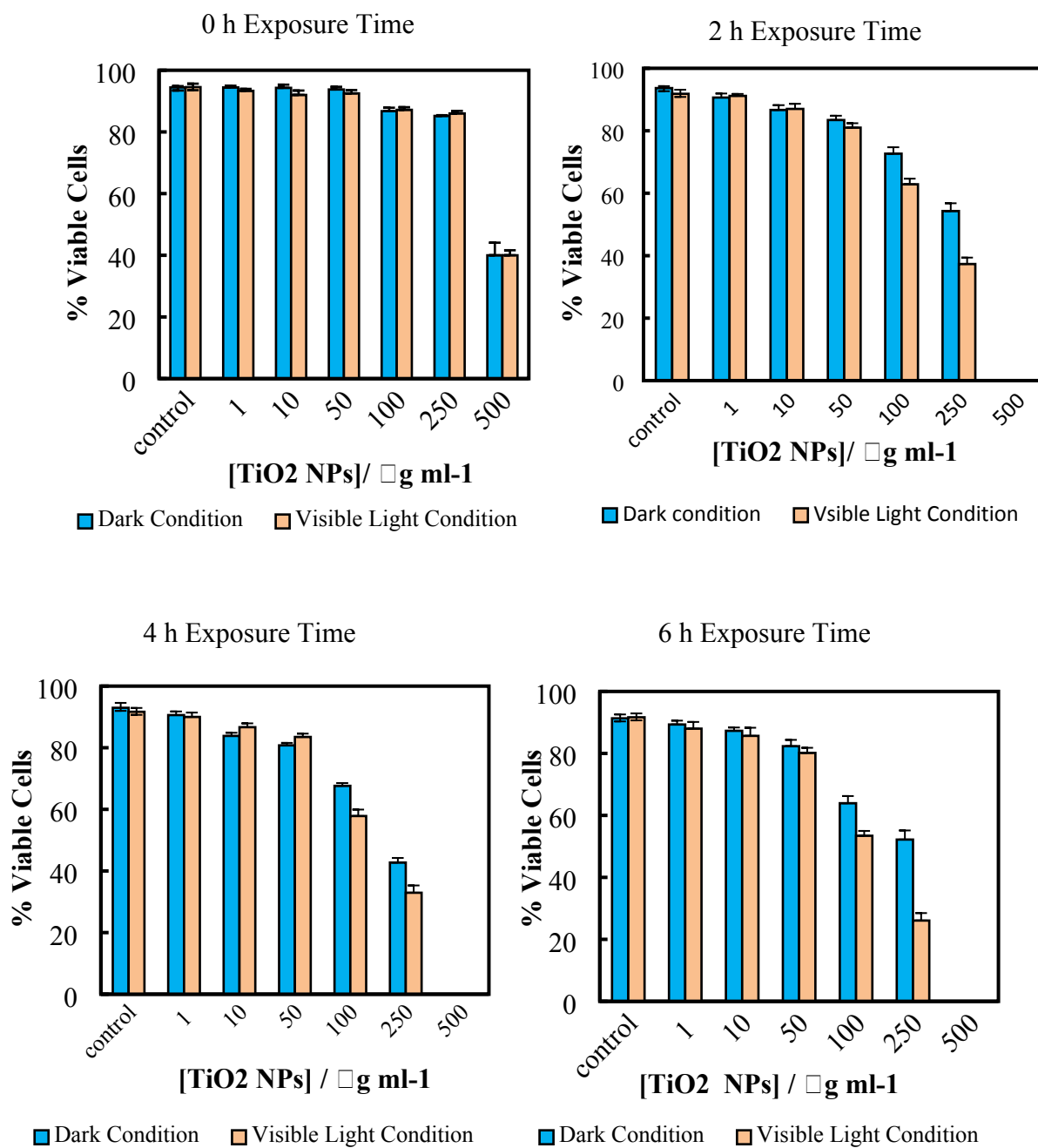


Figure S7: The viability of *C. Reinhardtii* cells incubated with different concentrations of TiO₂NPS at pH 4 in dark conditions and in visible light at 0h, 2 h, 4 h and 6 h exposure times compared with the control sample.

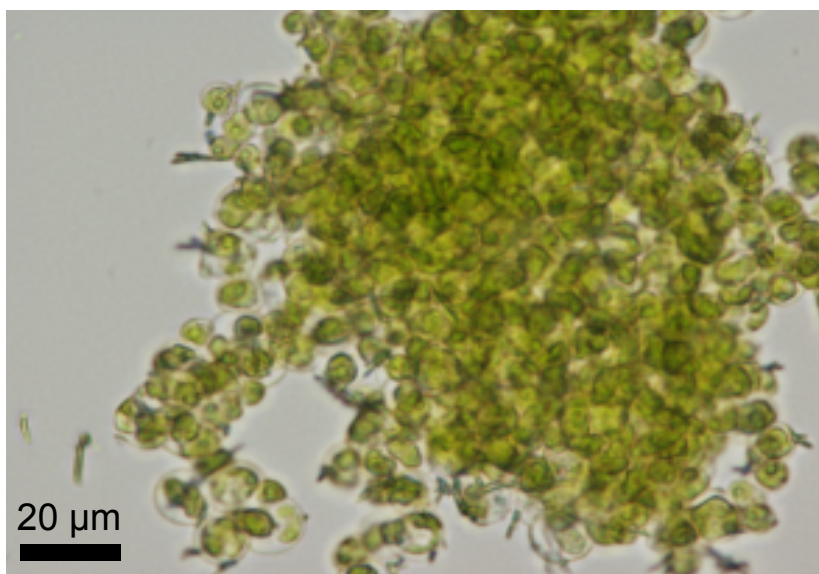


Figure S8: The 50x bright field microscopic image of aggregated *C. Reinhardtii* at high concentration of TiO₂NPs.

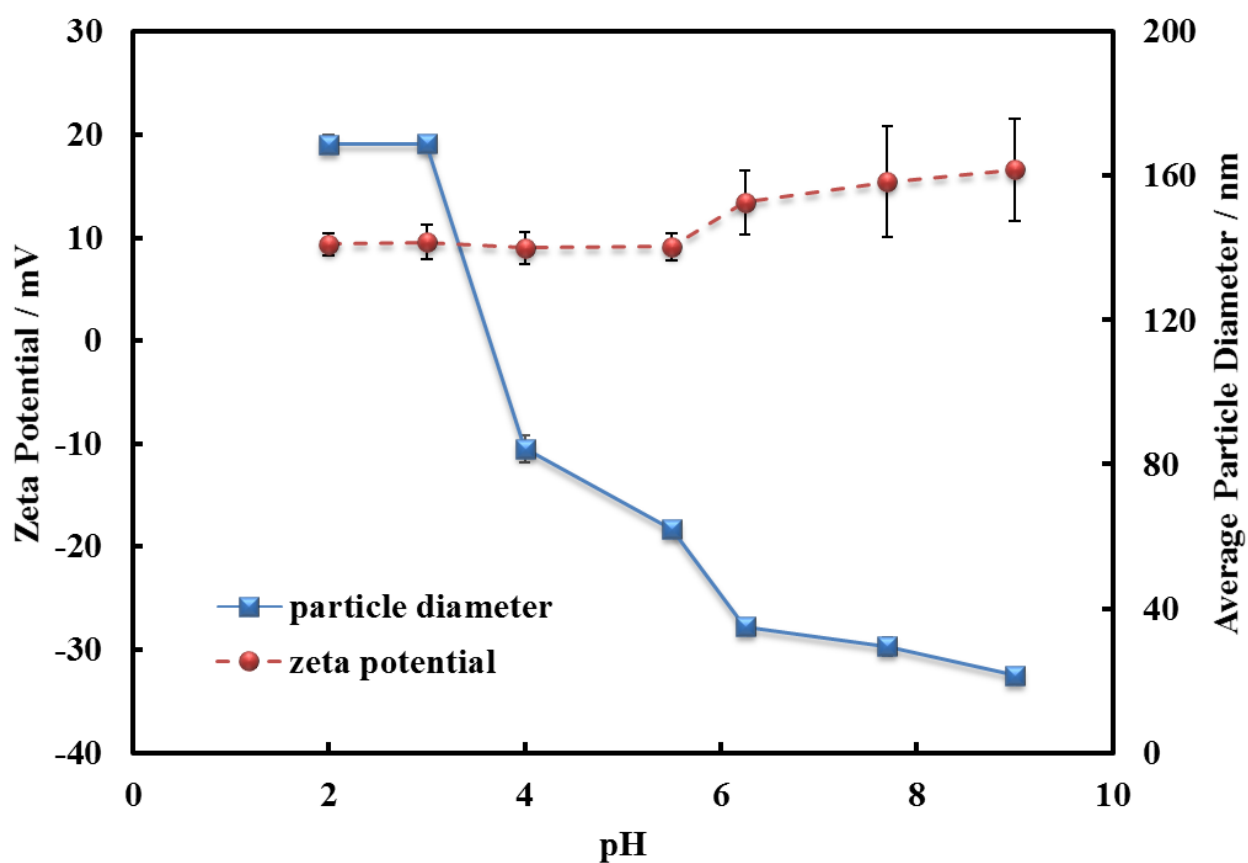


Figure S9: The variation the zeta potential and the particle diameter of dispersed rutile TiO₂NPs in an aqueous solution of 1 mM of NaCl as a function of pH which was adjusted by addition of small amount of aqueous solutions of 1M HCl or 1M NaOH. The square symbols show the effect of pH on the average particle hydrodynamic diameter while the circle symbols represent the particle zeta potential vs. pH.

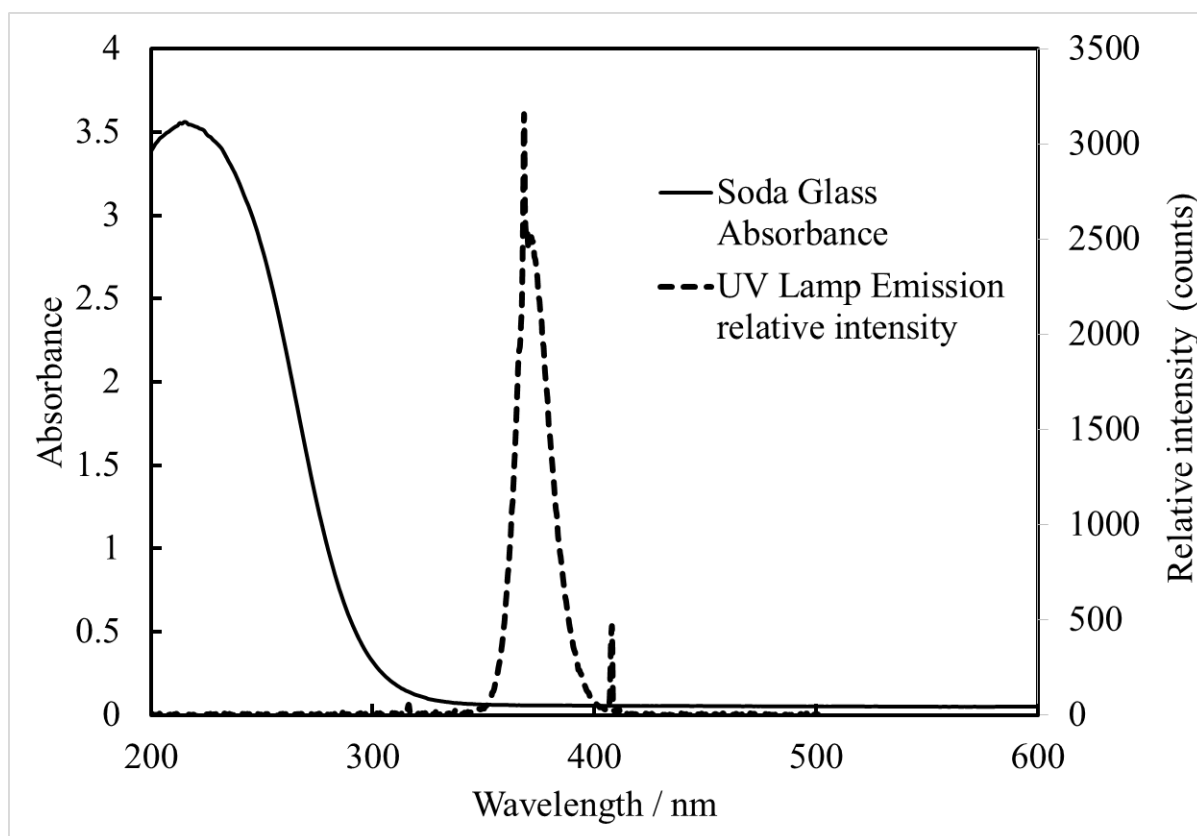


Figure S10: LHS axis: The absorbance spectrum of the soda glass tubes used for the incubation of the cell with TiO₂NPs in UV light. RHS axis: The emission spectrum of the UV lamp which refers to that the maximum emission occurs at 365 nm which was measured by USB4000-UV-VIS detector (Toshiba TCD1304AP Linear CCD array, USA). This UV light source was used to irradiate *C. Reinhardtii* and yeast in the presence of TiO₂NPs.

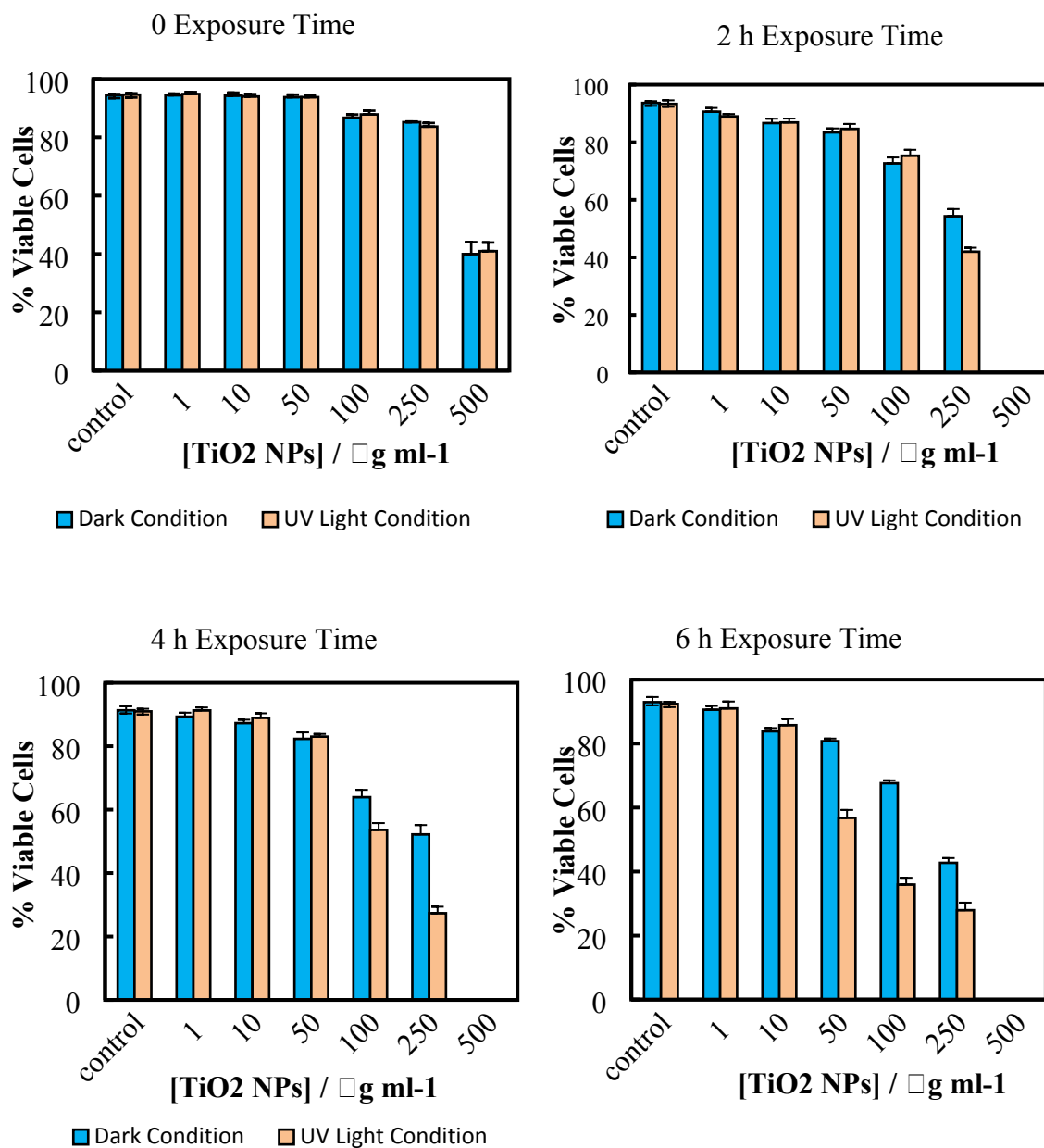


Figure S11: The viability of *C. Reinhardtii* cells incubated with different concentrations of TiO₂NPs in the presence of UV light at 0 h, 2 h, 4 and 6 h exposure times against the control sample.

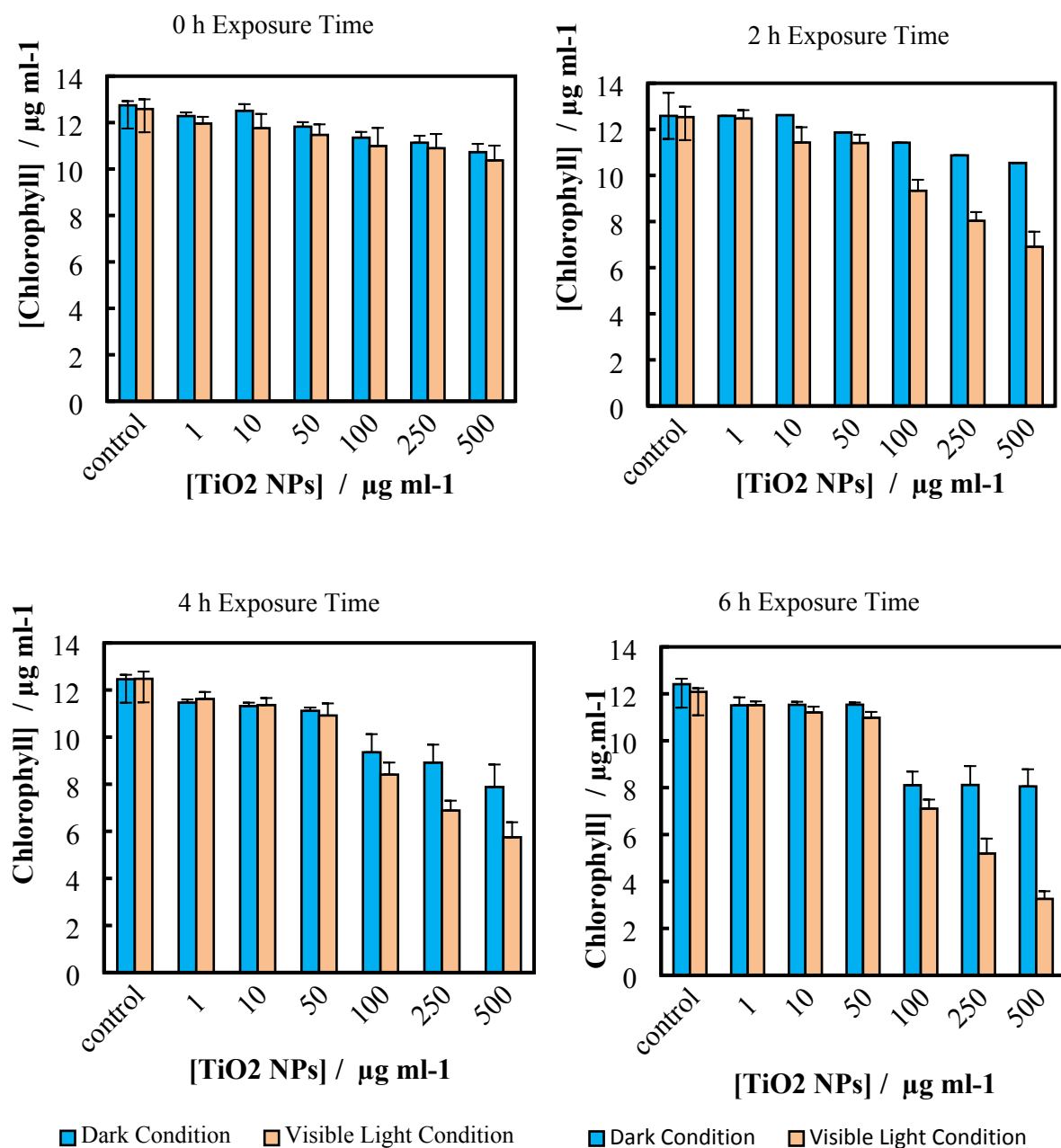


Figure S12: Chlorophyll content in *C. Reinhardtii* versus TiO₂NPs concentration at 0 h, 2 h, 4 h and 6 h exposure times as an evidence of viable cells in dark conditions and upon exposure to visible light.

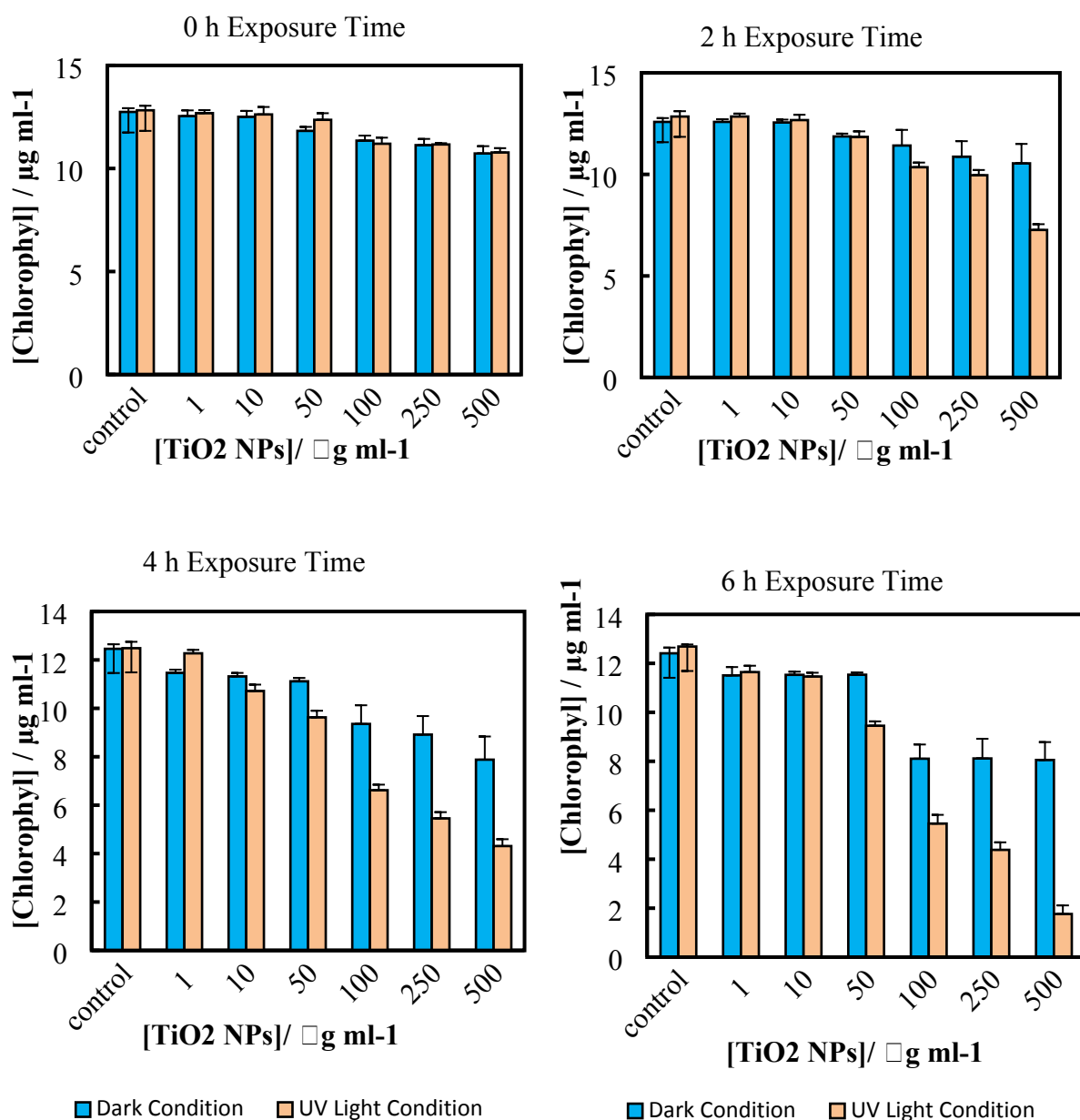
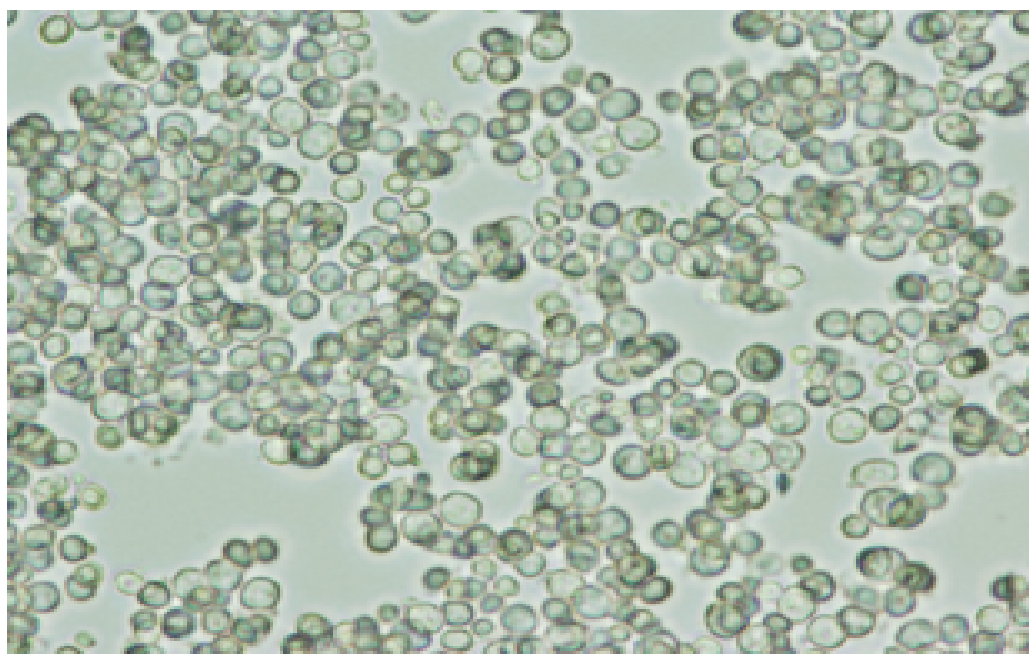
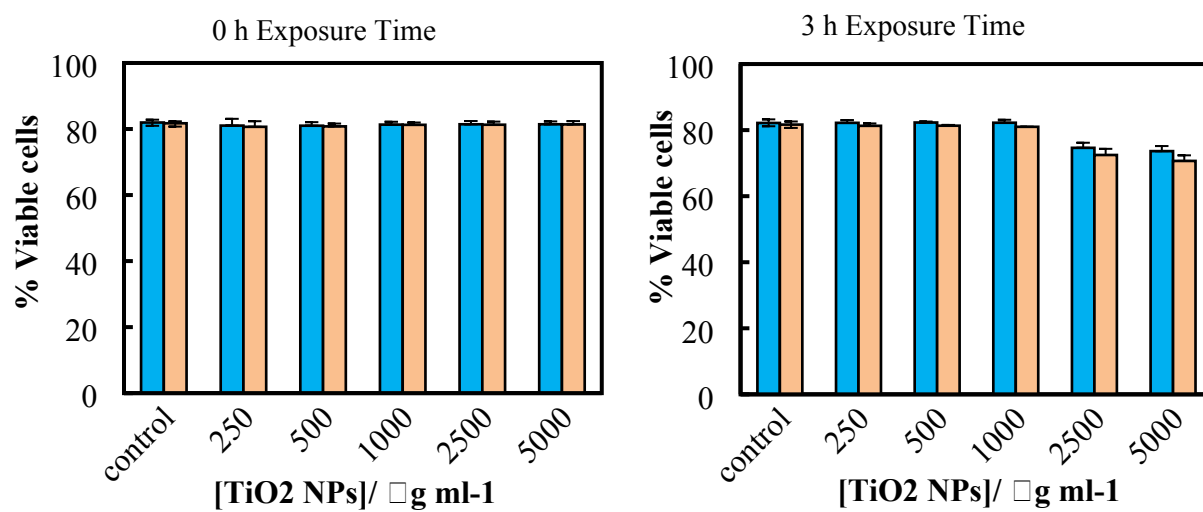


Figure S13: Chlorophyll content in *C. Reinhardtii* algae after UV-irradiation in the presence of various concentrations of TiO_2NPs in comparison with dark conditions.



20 μm

Figure S14: Optical image of yeast cells incubated with 3000 $\mu\text{g mL}^{-1}$ TiO_2NPs .



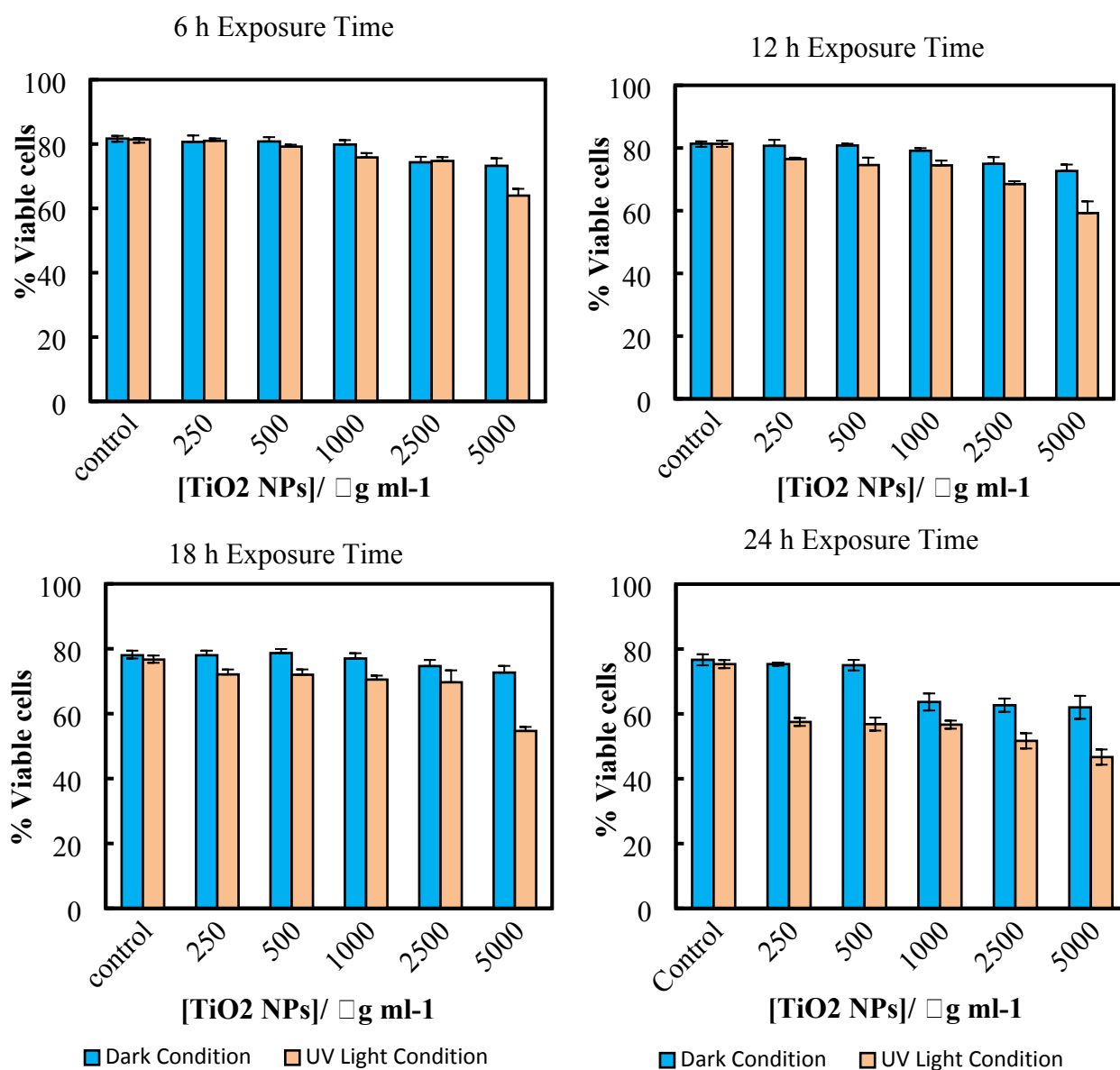


Figure S15: The percentage of viable yeast cells after incubation with TiO₂NPs of different concentration in the presence of UV light and in dark conditions at exposure times varying from 0 h to 24 h. The data show higher toxic effect of the TiO₂NPs in UV light than in dark conditions which can be attributed to the production of reactive oxygen species in the presence of atmospheric oxygen.

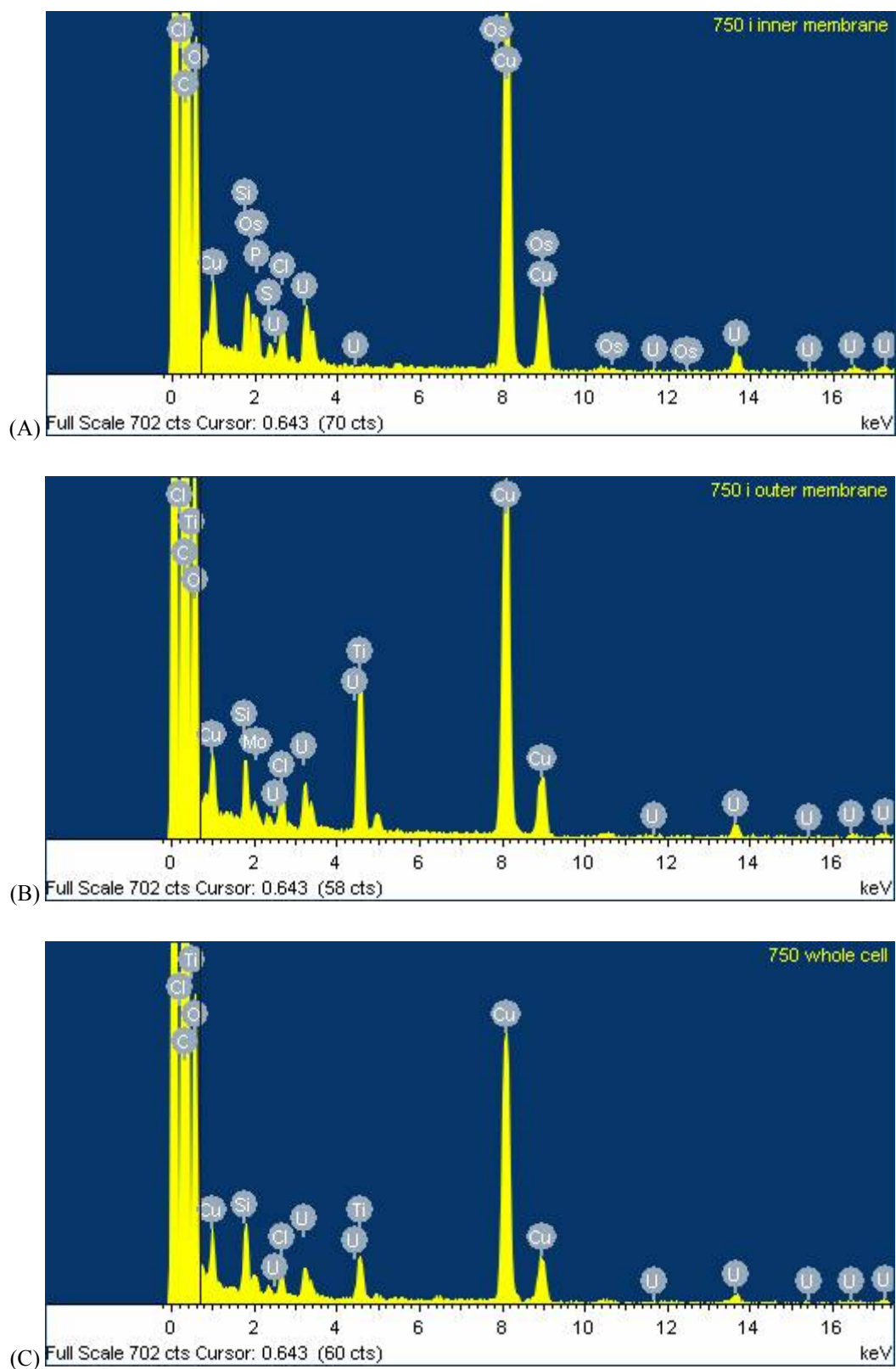


Figure S16: EDX diagram of the *C. Reinhardtii* algae cell at 750 ppm: (A) cell interior membrane and (B) cell outer membrane regions; (C) whole cell. The data indicate the absence of Ti in the cell interior but show its presence on the cell outer membrane. This demonstrates the lack of internalised TiO₂NPs in *C. Reinhardtii* even at NPs concentration 750 ppm.

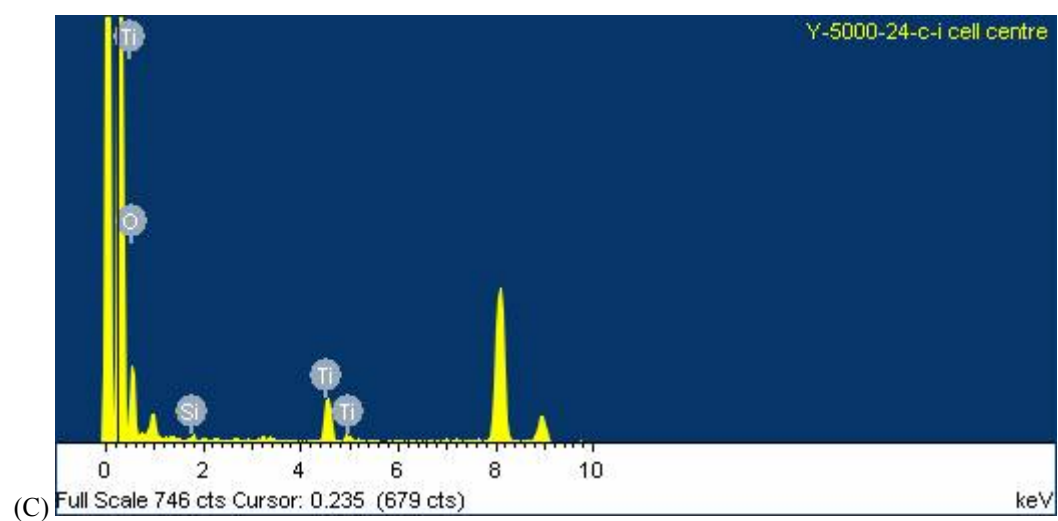
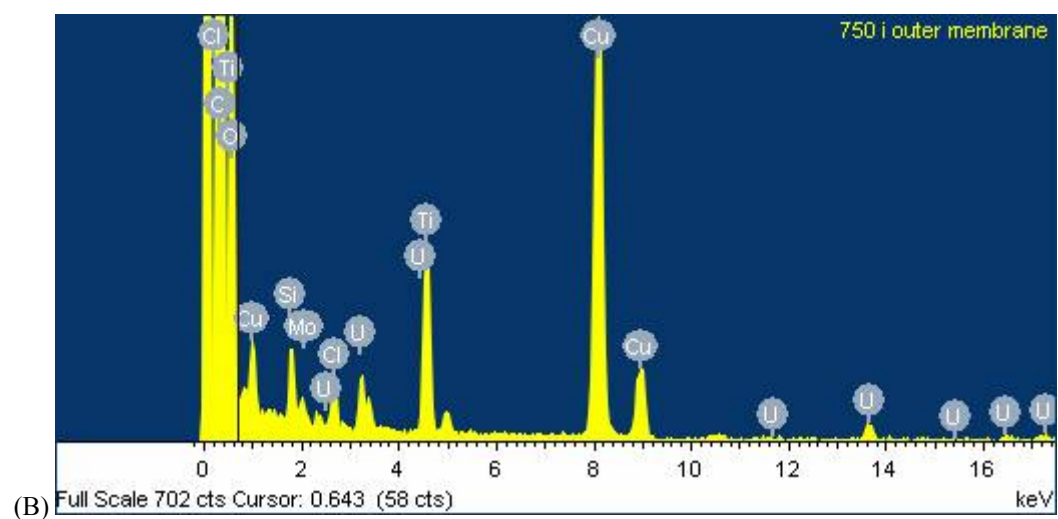
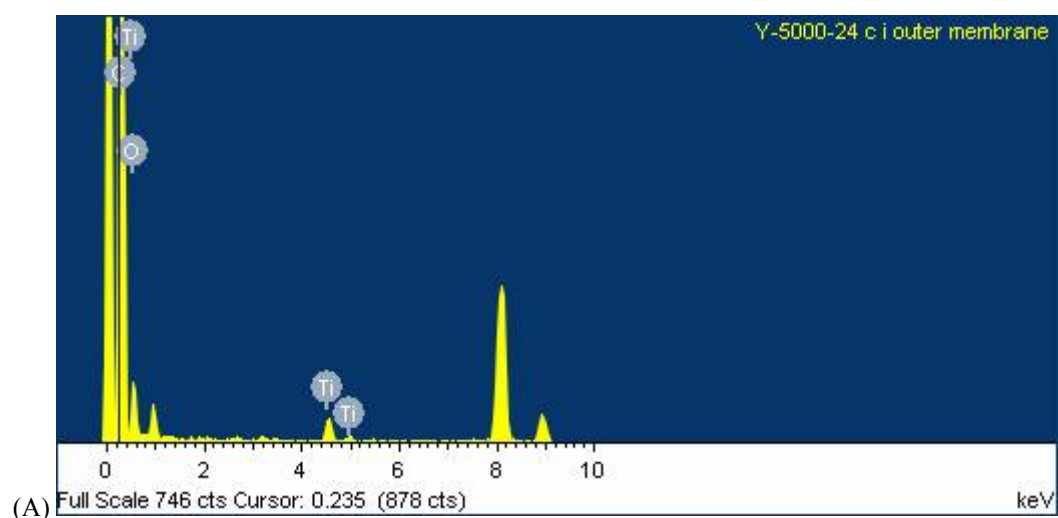


Figure S17: EDX diagram of yeast cell at 1000 ppm: (A) cell interior membrane and (B) cell outer membrane regions; (C) the cell centre. The data indicate the presence of TiO₂NPs both on the outer and the inner part of the cell membrane. This confirms the internalised TiO₂NPs in yeast at this NPs concentration.